ACS OMEGA

Open Access

http://pubs.acs.org/journal/acsodf

Article

Single-Walled Carbon Nanotube-Modified Gold Leaf Immunosensor for *Escherichia coli* Detection

Sara Joksović,* Ivana Kundačina, Ivana Milošević, Jovana Stanojev, Vasa Radonić, and Branimir Bajac

Cite This: *ACS Omega* 2024, 9, 22277−22284

Read Online

ACCESS | Metrics & More | Article Recommendations

ABSTRACT: The requirement to prevent foodborne illnesses underscores the need for reliable detection tools, stimulating biosensor technology with practical solutions for in-field applications. This study introduces a low-cost immunosensor based on a single-walled carbon nanotube (SWCNT)-modified gold leaf electrode (GLE) for the sensitive detection of *Escherichia coli*. The immunosensor is realized with a layer-by-layer (LbL) assembly technique, creating an electrostatic bond between positively charged polyethylenimine (PEI) and negatively charged carboxyl-functionalized SWCNTs on the GLE. The structural and functional characterization of the PEI-SWCNT film was performed with Raman spectroscopy, high-resolution scanning electron microscopy (HRSEM), and electrical measurements. The PEI-SWCNT film was used as a substrate for antibody immobilization, and the electrochemical sensing potential was validated using electrochemical impedance spectroscopy (EIS). The results showed a wide dynamic range of *E. coli* detection, 10^1−10^8 cfu/mL, with a limit of detection (LOD) of 1.6 cfu/mL in buffer and 15 cfu/mL in the aqueous solution used for cleansing fresh lettuce leaves, affirming its efficiency as a practical and affordable tool in enhancing food safety.

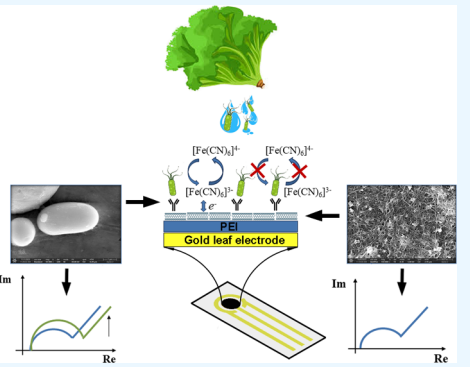

INTRODUCTION

The growing concern about food safety and bacterial contamination has become a prominent issue in the global market marked by increased food production, distribution, and consumption. The prevention of foodborne illnesses, often linked to bacterial contamination, requires safety screening and analyses across the entire food production continuum. One of the most common and persistent bacteria in the mineral soil, water sources, and subsequently after irrigation in fruits and vegetables is *Escherichia coli*.[1] Databases and studies across 10 out of the 14 World Health Organization (WHO) subregions revealed a global annual incidence of 2.8 million cases.[2] *E. coli* has emerged as a significant health threat, playing a substantial role in diarrheal diseases, urinary tract infections, sepsis, meningitis, and pyelonephritis, even in developed countries.[3] In this sense, reliable and cost-effective tools for the sensitive detection of contaminating pathogens are required to ensure food safety.[4,5]

Biosensor technology has rapidly emerged as a progressive field in modern science, combining the expertise from diverse disciplines to create innovative sensing devices applicable in food safety, environmental monitoring, and public health domains.[6] Biosensors hold the potential to develop cost-effective portable devices with rapid quantification of the present bacteria with high specificity and sensitivity in small volumes of a liquid sample.[7] They are promising alternatives to traditional methods, such as culture techniques, or molecular biology methods, such as the polymerase chain reaction (PCR), which require expensive laboratory equipment, skilled personnel, and specific conditions. Recent studies in the field of biosensor technology have proposed solutions based on optical,[8] colorimetric,[9] mass-change,[10] and electrochemical detection principles.[11] With their high sensitivity, rapid detection, and in-field application potential, electrochemical biosensors based on potentiometric, conductometric, and impedimetric principles are proposed for different applications in food safety.[12]

Our recent study introduced a low-cost fabrication technology of gold electrodes using gold leaves.[13] The novel technology confirmed the sensitivity, stability, and reproducibility of the electrodes, and consequently electrochemical signals. Finally, the potential in biosensing applications was demonstrated via development of an immunosensor for *E. coli* detection without any surface modification or signal amplification of gold leaf electrodes (GLEs).

Recent studies have widely used different nanomaterials and signal amplification strategies[14,15] in combination with various biorecognition elements for specific target detection. Namely,

Received: February 19, 2024
Revised: April 10, 2024
Accepted: April 26, 2024
Published: May 9, 2024

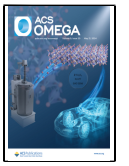

nanomaterials behave like a substrate for biorecognition element immobilization with a high specific surface area, while at the same time they act as transduction elements, improving the signal strength. Since the discovery of single-walled carbon nanotubes (SWCNTs) in 1993,[16] they have quickly become a worldwide focus of research due to their outstanding properties. With an ultrahigh surface area, excellent mechanical strength, high thermal and electrical conductivity, stability in various solutions, and outstanding electrochemical properties, SWCNTs have attracted attention for their potential application in biosensors.[17−20] The electrical properties of SWCNTs are widely known for their susceptibility to change when exposed to biomolecules, and for this reason, CNT-based biosensors are attractive to many research groups around the world. So far, various types of CNT-based biosensors are proposed in the literature, such as SWCNT-based biosensors for the detection of essential vitamins (e.g., ascorbic acid) or dopamine,[19] CNT-based electrochemical enzyme sensors for the detection of glucose and choline,[21−23] electrochemical DNA sensors for the immobilization of nucleic acid[24] and RNA,[25,26] electrochemical immunosensors also based on CNTs for the detection of mycotoxins[27] and various types of cancer,[28−30] etc.

In order to increase the electroactive surface of an electrochemical biosensor, a novel approach based on nanomaterial modification is examined in this research. We propose a low-cost SWCNT-based GLE immunosensor for the sensitive detection of *E. coli* in the liquid medium collected after cleansing lettuce. For the fabrication of the immunosensor, a layer-by-layer (LbL) assembly technique has been used for alternate deposition of the positively charged layer of PEI and negatively charged carboxyl-functionalized SWCNTs (SWCNTs-COOH) on the GLE to form an electrostatic bond between the layers. The SWCNT-based film has been characterized with Raman spectroscopy and HRSEM in terms of structural properties, while the change in the electrical response and electrochemical properties is examined through the sensor's fabrication steps and final testing for the detection of spiked *E. coli* in samples of water used for cleansing fresh lettuce leaves.

EXPERIMENTAL SECTION

Materials and Methods. *Materials and Chemicals.* For GLE fabrication, 125 μm thick poly(vinyl chloride) (PVC) sheets (ImageLast A4 125 Micron Laminating Pouch) were purchased from Fellowes Brands (Poland), commercial gold leaves were obtained from Belgrade (Serbia), while poly-(tetrafluoroethylene) (PTFE) spray was purchased from Wurth (Serbia). Commercial carboxyl-functionalized single-walled carbon nanotubes (SWCNTs-COOH, purity: >90%, diameter: 4−5 nm, length: 0.5−1.5 μm), polyethylenimine (PEI) solution ($M_n \sim 60{,}000$, $M_w \sim 750{,}000$), bovine serum albumin (BSA), potassium ferricyanide (K3[Fe(CN)6]), potassium ferrocyanide (K4[Fe(CN)6]), and tryptone soya agar (TSA) were purchased from Sigma-Aldrich, while rabbit polyclonal anti-*E. coli* antibody (ab137967) was purchased from Abcam (USA). Deionized (DI) water was used during the whole experiment.

Equipment. For GLE manufacturing, a Laminator PDA3 330C (PINGDA, China) and a Nd:YAG laser PowerLine D-100 (Rofin-Sinar, Germany) were used. Structural characterization was performed with a Horiba XploRA PLUS Raman spectrometer (green laser, λ = 532 nm) and a Thermo Fisher Scientific Apreo C high-resolution scanning electron microscope. Electrical properties were investigated with a semiconductor parameter analyzer (range: from −1 to 1 V, step by 0.01 V), while electrochemical characterization was done with a potentiostat/galvanostat/impedance analyzer, PalmSens4 (PalmSens BV, Houten, The Netherlands) and PSTrace 5.8 software.

Experimental Procedure. The experimental part will be divided into 6 sections: (i) gold leaf electrode (GLE) fabrication, (ii) PEI-SWCNT film preparation on a gold leaf electrode (GLE), (iii) immunosensor construction, (iv) bacteria cultivation and quantification, (v) validation of biosensing performances, and (vi) fitting results with the equivalent Randles circuit.

GLE Fabrication. The GLE fabrication procedure is described in detail in our previous work.[13] Briefly, two layers of gold leaf sheets were laminated by the hot lamination process at the surface of PVC supporting layers. Afterward, laser ablation was used for removing the gold from the surface, leaving only gold parts that create the electrode design.

PEI-SWCNT Film Preparation. As in our previous work,[31,32] we used a simple, low-cost LbL technique to fabricate a CNT-based biosensor. The principle of the LbL technique is based on the alternate deposition of positively and negatively charged layers to form a thin monolayer film. The prepared 1% PEI solution served as the positively charged layer, while the 0.1% dispersion of SWCNTs-COOH served as the negatively charged layer. The detailed procedure of biosensor realization is shown in Figure 1. In the first step, GLE was cleaned in 0.5 M sulfuric acid by cyclic voltammetry (potential range: 0−1.5 V vs gold reference electrode, scan rate: 0.5 V/s, 10 scans) and then washed with DI water (Figure 1). Subsequently, a 0.6 μL droplet of PEI solution and a 0.6 μL droplet of SWCNTs-COOH dispersion were added, with the washing step in between. The PEI-SWCNT film has a bilayer structure, as shown in Figure 1. The prepared bilayer structure was dried at room temperature, characterized in terms of electrical and electrochemical properties, and used for biosensor preparation.

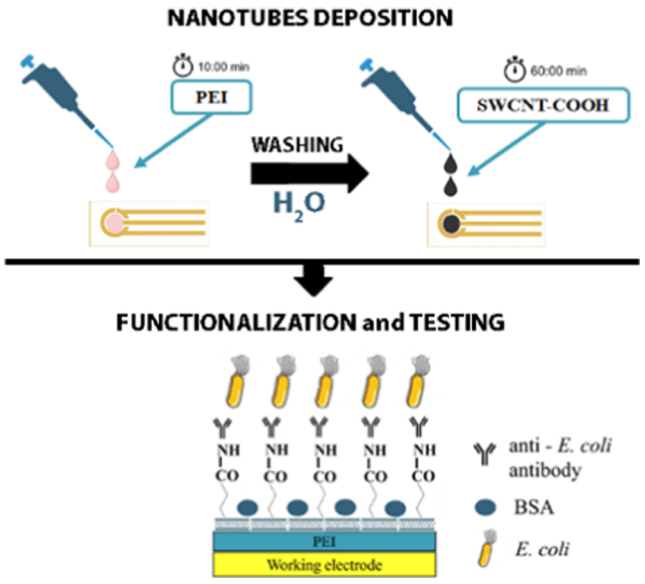

Figure 1. Schematic view of the layer-by-layer (LbL) procedure and functionalization steps.

https://doi.org/10.1021/acsomega.4c01599
ACS Omega 2024, 9, 22277−22284

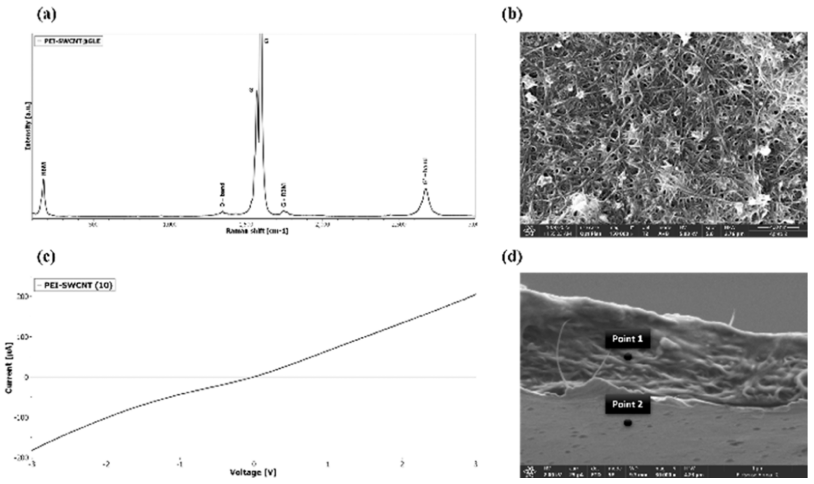

Figure 2. (a) Raman spectra of the PEI-SWCNT film on a gold leaf electrode (GLE); (b) micrograph of the PEI-SWCNT@GLE surface at 150,000× magnification; (c) current−voltage dependence of a PEI-SWCNT film; and (d) cross section of PEI-SWCNT@GLE.

Immunosensor Construction. Surface functionalization with antibodies of SWCNT-modified GLE implies a 1 h incubation of 0.1 mg/mL anti-*E. coli* antibodies on the working electrode, i.e., on the PEI-SWCNT film. Namely, carboxyl groups of SWCNTs covalently bind to amino groups of antibodies, making a biorecognition layer on the SWCNT surface. Afterward, the electrode was rinsed with DI water, and incubation of 50 μg/mL BSA was done for 20 min to prevent nonspecific binding on the surface (Figure 1d). Finally, each concentration of bacteria was incubated for 20 min and characterized via EIS (frequency was set in the range 1 Hz−100 kHz with an amplitude of 10 mV, direct potential was equal to zero, and measurements were performed versus open-circuit potential in the two-electrode system).

Bacteria Cultivation and Quantification. Bacteria were prepared by overnight culturing at 37 °C on TSA plates, while different concentrations in the range of 10^1−10^5 cfu/mL were made from 0.5 McFarland standard. Besides specific *E. coli* (ATCC 25922) bacteria, the specificity of detection was confirmed with two nonspecific bacteria, Gram-positive *Bacillus subtilis* (PY79) and Gram-negative *Enterobacter aerogenes* (ATCC 13048). Specificity tests with nonspecific bacteria were performed with 10^4 cfu/mL. Counting of bacterial colonies was performed on TSA plates to confirm the bacterial concentrations. A similar procedure was used for spiked *E. coli* in the complex matrix of the aqueous solution employed for lettuce cleansing.

Validation of Biosensing Performances. Each concentration of bacteria was incubated for 20 min, rinsed with DI water, and characterized with a redox probe (5 mM mix of potassium ferro/ferricyanide prepared in DI water) via EIS. Biosensing performances were validated in buffer solutions and samples of aqueous solution used for cleansing fresh lettuce with spiked bacteria.

For validation of performances in complex matrices, *E. coli* was spiked in the aqueous solution used for cleansing lettuce. Lettuce samples were purchased from a local supermarket and left in DI water for 1.5 h. The aqueous solution was filtered with a 0.2 μm sterile filter to prevent water contamination with bacteria. The filtered aqueous solution was used for both saturating the immunosensor surface and conducting control experiments, as nonspecific components in the sample could yield a false-positive signal. Finally, *E. coli* bacteria were spiked into aqueous solution samples, with a series of dilutions in the concentration range from 10^1 to 10^8 cfu/mL.

For validation of biosensing performances in lettuce aqueous solution samples, a control experiment was made with repeated incubations of the aqueous solution on separate electrodes, prepared with the same procedure as the tested one. Both electrodes were saturated with nonspecific components of lettuce aqueous solution during 2 h of incubation. In the following steps, the controlled electrode was tested with repeated incubations of lettuce aqueous solution, while the test one was tested with spiked *E. coli* in lettuce aqueous solution. In this way, a false-positive signal was avoided.

Fitting Results with the Equivalent Randles Circuit. The impedance results correspond to the behavior of the electronic circuit with different electronic components that illustrate the droplet−electrode interface. The redox probe is described with solution resistance Rsol, while the droplet−electrode interface is described with a parallel RC circuit. The RC circuit contains charge-transfer resistance R_{ct}, which directly quantifies centers of interactions available for the redox probe reaction at the electrode surface. With the increase of bacterial concentration, this parameter also increases, and it is used for the description of sensor saturation. Besides, the Warburg element is connected with the R_{ct} parameter and describes the diffusion process from the droplet to the electrode surface. Finally, R_{ct} and W are connected in parallel with a constant-phase element (CPE), which illustrates the double-layer properties of the interface between the electrode and the electrolyte in real systems with imperfect capacitors. The described circuit is known from the literature as the Randles circuit.[33] The open-source program EIS Spectrum Analyser was used to fit the results with an equivalent Randles circuit. The program is available at http://www.abc.chemistry.bsu.by/vi/analyser/.

RESULTS

This section interprets the structural and electrical properties of the PEI-SWCNT@GLE biosensor. Subsequently, the Discussion section will encompass the biosensor's functionalization process and its efficacy in detecting *E. coli*. The final segment will provide information on the biosensor's specificity and sensitivity for lettuce sample analysis.

Characterization of PEI-SWCNT@GLE. *Raman Spectroscopy.* Raman spectroscopy provided information about the

https://doi.org/10.1021/acsomega.4c01599
ACS Omega 2024, 9, 22277−22284

molecular structure of the carbon material. Figure 2a shows the PEI-SWCNT bilayer structure on a GLE, with the five most intense peaks describing the nanotubes. The most intense peak at 1595 cm^{-1} is a G-band, and it is divided into two sub-bands (G+ and G−). The shape of the peaks indicates the semiconducting behavior of nanotubes according to the literature.[34,35] The relatively low intensity of a D-band peak at 1345 cm−1 confirms the high quality of carbon nanotubes, as the D-band is known to indicate disorder in the structure.[34,35] The additional peak at 2677 cm^{-1} is known as the G′-band, and it originates from the defects. The radial breathing mode (RBM) vibration at 173 cm^{-1} confirms the fact that single-walled carbon nanotubes are present, as it is a specific vibrational mode that only occurs in single-walled carbon nanotubes.[34,35]

High-Resolution Scanning Electron Microscopy. High-resolution scanning electron microscopy (HRSEM) provided further details of the structure, morphology, and distribution of SWCNTs in the PEI matrix on a GLE. The micrograph in Figure 2b shows the surface of a PEI-SWCNT film on a GLE at 150,000× magnification, while the micrograph in Figure 2d represents the cross section. It can be observed that the distribution of SWCNTs is relatively uniform along the surface. The micrograph also shows that the structure of the film is porous, and the nanotubes are interconnected. The porous structure provides a high specific surface area, which should enable better sensitivity of the biosensors. A higher specific surface area means a larger surface area for antibodies and bacteria to bind to antibodies, resulting in enhanced signals. From Figure 2d, it can be observed that the film is continuous and that the nanotubes are embedded in the polymer matrix. To confirm the existence of the PEI-SWCNT film, energy-dispersive X-ray (EDX) analysis was performed (Table 1).

Table 1. EDX Analysis of the PEI-SWCNT Film and GLE

	net counts	
element	point 1 (PEI-SWCNT)	point 2 (GLE)
gold (Au)	183	6501
carbon (C)	8152	675
nitrogen (N)	558	13
oxygen (O)	656	129

Point 1 indicates the PEI-SWCNT film, while point 2 represents the GLE. The first point shows an increased net count of elements such as carbon (C), nitrogen (N), and oxygen (O). The predominance of carbon and oxygen is attributed to SWCNTs-COOH, while the presence of nitrogen indicates the incorporation of PEI polymers with amino ($-NH_2$) and imino (−NH−) groups. The increased net count of gold in point 2 indicates that this area is predominantly gold.

Current−Voltage Characteristics. As mentioned in the Materials and Methods section, the electrical $I-V$ characterization of the PEI-SWCNT film was performed using a semiconductor parameter analyzer, and the result is shown in Figure 2c. It can be noticed that the current−voltage dependence is almost linear, which means that the film has an Ohmic behavior.

Calibration, Sensitivity, and Specificity of the Immunosensor for Lettuce Samples. Figure 3a presents the electrochemical confirmation of each functionalization step after adding the PEI-SWCNT film, antibodies, and BSA at the bare GLE surface. It can be seen that the PEI-SWCNT film decreases the impedance significantly, which confirms the conductive properties and efficient electron transfer through the deposited film. On the other hand, antibodies and BSA block the electron transfer between the film and the redox probe, which is confirmed as an impedance increase in the graph. Following surface functionalization, the immunosensor was exposed to an increased concentration of bacteria, which is confirmed with HRSEM (Figure 3b).

The immunosensor performance was validated initially in phosphate-buffered saline (PBS) in order to make a calibration curve of the immunosensor's response to increasing concentrations of bacteria in the PBS buffer. Figure 4a presents Nyquist diagrams of the immunosensor's response for the *E. coli* concentration in the range 10^1-10^5 cfu/mL. The Randles circuit used for fitting results is presented in the inset of Figure 4b, and the R_{ct} parameter is extracted for each concentration response. The calibration curve in Figure 4b shows a linear increase of charge-transfer resistance as a function of *E. coli* concentration with excellent linear properties (R^2 = 0.97). Figure 4c shows results of specificity tests with specific *E. coli* and two nonspecific bacteria, *B. subtilis* and *E. aerogenes*. Results are presented as a relative change of the signal versus BSA-functionalized R_{ct} parameters following the equation: $\delta(\%) = 100 \times [R_{ct(bacteria)} - R_{ct(BSA)}]/R_{ct(BSA)}$. It can be seen that the signal for nonspecific bacteria is negligible in comparison with that for specific *E. coli*.

Figure 4d presents results of the control experiment of repeated incubations of lettuce aqueous solution at the electrode surface. The results show that the signal after a slight increase has a constant response, which confirms electrode saturation with nonspecific components from lettuce aqueous solution. On the other hand, Figure 4e shows a signal increase for spiked *E. coli* bacteria in lettuce aqueous solution

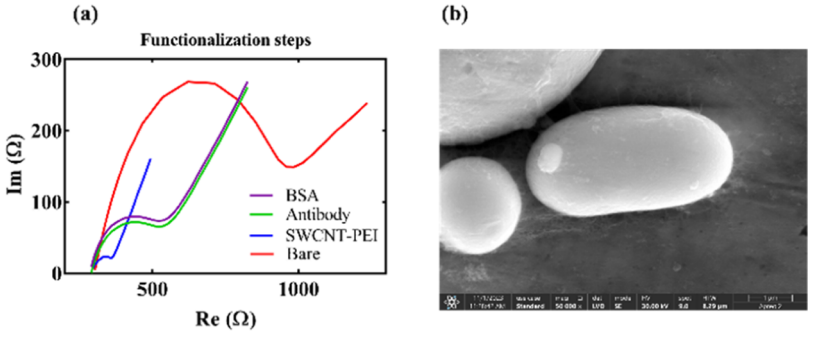

Figure 3. (a) Nyquist diagrams for functionalization steps; (b) SEM image of bacteria on the GLE-SWCNT surface at a magnification of 50,000x.

https://doi.org/10.1021/acsomega.4c01599
ACS Omega 2024, 9, 22277−22284

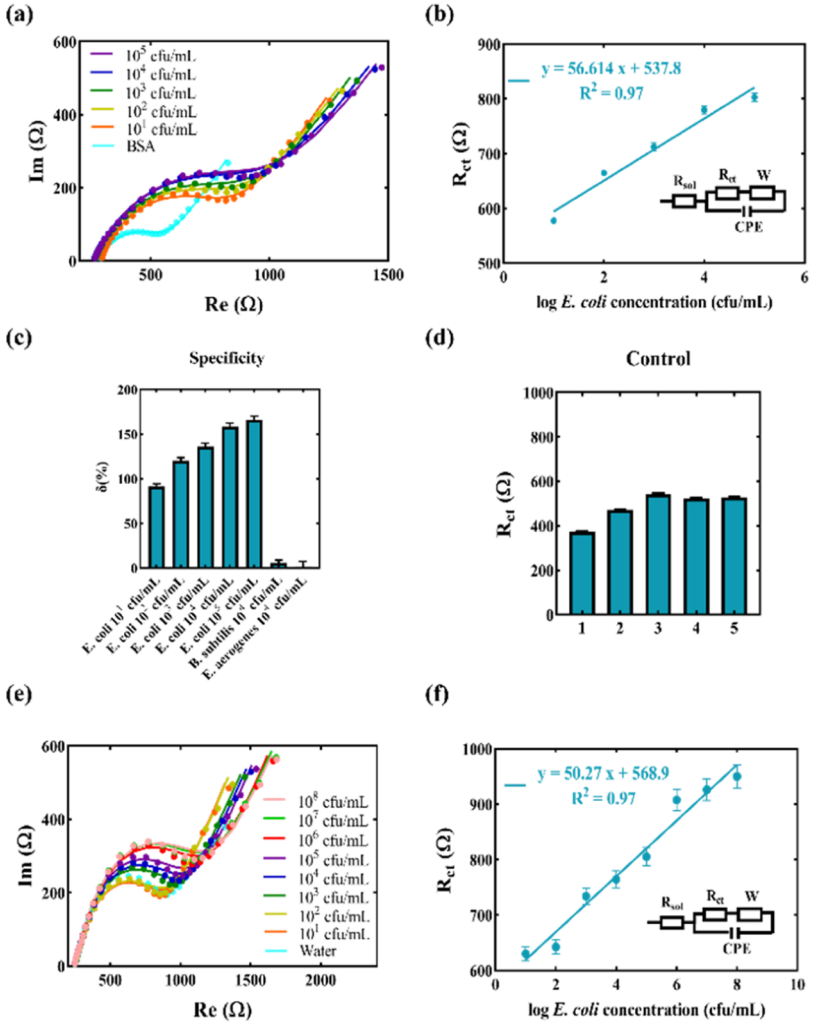

Figure 4. (a) Nyquist diagrams for *E. coli* detection in PBS; (b) calibration curve of charge-transfer resistance as a function of *E. coli* concentration; (c) specificity tests for nonspecific *B. subtilis* and *E. aerogenes*; (d) control measurements—repeated incubations of lettuce aqueous solution at the immunosensor surface; (e) Nyquist diagrams for spiked *E. coli* in lettuce aqueous solution; (f) calibration curve of charge-transfer resistance as a function of spiked *E. coli*.

samples in the concentration range 10^1–10^8 cfu/mL, which additionally confirms the specificity of the proposed immunosensor. The charge-transfer parameter as a function of *E. coli* concentration shows a linear increase with excellent linear properties (R^2 = 0.97) (Figure 4f).

Discussion. This study presents a cost-effective and efficient way of realizing an immunosensor for the detection of *E. coli*. As was described, the working electrode of GLE was used as a substrate for deposition of the PEI-SWCNT film, which enables the formation of a biorecognition layer by binding antibodies at the free carboxyl groups of SWCNTs.

The LbL assembly technique proves to be cost-effective and versatile, demonstrating adaptability to various substrates[31] and enabling precise control over layer deposition with small amounts of material. The detailed characterization of the PEI-SWCNT film with Raman spectroscopy and HRSEM verified the presence of SWCNTs and PEI in the samples.

HRSEM images further showed the formation of SWCNT network interconnected with PEI with high surface area and porosity, which increases the electroactive surface, important for high electrochemical signals. Additionally, the HRSEM image showed that the network pore size is in the range of dozens of nm. In the case of bacteria that have size in the range of microns, the pores need to be smaller than the target in order to avoid the sticking of nonspecific bacteria in the film and thereby their false-positive contribution to the signal. On the other hand, the linearity of current–voltage characteristics confirmed the film stability and uniform electrical conductivity without a nonlinear or complex behavior. This characteristic enables predictable and controllable electrical responses, which are important for sensor construction.

Electrochemical results confirmed the high sensitivity and excellent linearity in both PBS buffer samples and complex matrix samples. In addition, specificity tests confirmed the excellent specificity of the proposed immunosensor with a high signal, even for low concentrations of bacteria. This confirms the low signal-to-noise ratio of the proposed sensor with high reliability for detecting bacteria.

The LOD was estimated to be 1.6 cfu/mL according to the IUPAC formula $3\sigma/d$[36] (where σ represents the standard deviation of the blank and d is the slope of the linear calibration curve) in the PBS buffer, while the LOD in lettuce aqueous solution was calculated to be 15 cfu/mL. The results show that the LOD is higher in the complex matrix, which can also be noticed from slopes of charge-transfer resistance (Figure 4b,f), since saturation of the surface with nonspecific

https://doi.org/10.1021/acsomega.4c01599
ACS Omega 2024, 9, 22277–22284

Table 2. Comparison of the Proposed Immunosensor with Other Biosensors from the Literature for Bacterial Detection in Leafy Vegetables

sensor material and technology	detection technique	biorecognition element	detection time	LOD [cfu/mL]	dynamic range [cfu/mL]	bacteria	refs
e-beam deposition of Pt	EIS	aptamer	15 min	48	10^1–10^6	*Listeria spp.*	38
GCE modified with Si@MB and Au NPs	DPV	aptamer	30 min	2.6	10^2–10^7	*L. monocytogenes*	39
SWCNT-modified SPE	DPV	bacteriophage	1 h	1	1–10^4	*E. coli*	40
PEI-SWCNT-modified GLE	EIS	antibody	20 min	1.6 buffer/15 real sample	10^1–10^8	*E. coli*	this work

components of lettuce aqueous solution blocked some of the active binding sites for specific bacteria. However, the difference in the sensing performances still satisfies the detection of infective doses of *E. coli* of 10^2 cells.[37] In addition, the proposed solution based on the PEI-SWCNT film on the GLE surface showed 20% lower LOD in comparison with our previous work,[13] where the GLE immunosensor was used without any nanomaterial modification with a bigger surface of the working electrode (radius, 2.5 mm). Besides, the proposed PEI-SWCNT showed a signal enhancement and therefore better sensitivity and specificity with the signal change for almost 100% for low concentrations of bacteria (Figure 4c), which is 60% better than that in our previous work.

In general, electrochemical biosensors for the detection of bacteria from lettuce or leafy vegetables are rare in the literature. Recently proposed solutions use aptamers as a biorecognition element for specific detection of *E. coli* or *Listeria*, as these bacteria are commonly found in contaminated leafy vegetables. An aptasensor is developed using platinum electrodes fabricated using e-beam lithography for the detection of Listeria spp. in hydroponic lettuce growth media.[38] In another recent study, glassy carbon electrodes (GCEs) were modified with silicon, methylene blue (Si@MB), and gold nanoparticles (Au NPs) for the detection of *Listeria monocytogenes* in lettuce.[39] Besides, a biorecognition element based on a genetically engineered bacteriophage was used for the modification of SWCNT-modified screen-printed electrodes (SPE) and *E. coli* detection in spinach leaf samples.[40] However, this solution requires a pre-enrichment step, which increases the complexity of the procedure and the detection time. Table 2 compares all relevant parameters like LOD, dynamic range of detection, and detection time of the previously mentioned biosensors with the proposed PEI-SWCNT-modified GLE immunosensor.

In comparison with other proposed solutions, the proposed immunosensor based on GLEs modified with PEI-SWCNT films overcomes other solutions in terms of fabrication simplicity and price. The substrate (i.e, GLE) price is 10 times lower in comparison with other commercially available electrodes, like SPE made by companies Metrohm,[41] PalmSens,[42] etc. Although the carboxyl-functionalized SWCNTs can be a costly component of the sensor, for the film preparation, only small volumes were used (in the range of μL), which do not increase the final price significantly. The proposed immunosensor showed a performance comparable to those of existing solutions, exhibiting equivalent sensitivity with respect to the LOD and dynamic range while maintaining a similar detection time. On the other hand, the proposed immunosensor enables direct detection of bacteria in the sample without any labeling steps. In addition, the proposed solution can be easily adapted for other types of bacteria with other antibodies or any amino-modified biorecognition elements. In conclusion, the proposed immunosensor demonstrates superior performance in terms of fabrication simplicity and affordability with better or equally good sensing performance when compared to existing solutions.

CONCLUSIONS

In this study, a cost-effective immunosensor for *E. coli* detection was proposed based on a PEI-SWCNT-modified GLE. The results of Raman spectroscopy and HRSEM demonstrated the porous structure of the PEI-SWCNT film with a high surface area, increasing the electroactive efficiency. The Ohmic behavior in current–voltage characteristics confirmed the film stability and uniform electrical conductivity, while electrochemical results showed high sensitivity and specificity, with LODs of 1.6 cfu/mL in PBS buffer and 15 cfu/mL in lettuce aqueous solution. The proposed immunosensor showed an enhanced signal even for low concentrations of bacteria by using SWCNTs' conductive properties while at the same time having a suitable price, making it a good candidate for highly sensitive detection without the need for pre-enrichment steps; its adaptability to different biorecognition elements further enhances its versatility, offering an efficient and economical solution for bacterial detection in leafy vegetables.

AUTHOR INFORMATION

Corresponding Author

Sara Joksović – *University of Novi Sad, BioSense Institute, 21000 Novi Sad, Serbia;* orcid.org/0000-0002-7642-9917; Phone: +381652711526; Email: sara.joksovic@biosense.rs

Authors

Ivana Kundačina – *University of Novi Sad, BioSense Institute, 21000 Novi Sad, Serbia*

Ivana Milošević – *University of Novi Sad, BioSense Institute, 21000 Novi Sad, Serbia*

Jovana Stanojev – *University of Novi Sad, BioSense Institute, 21000 Novi Sad, Serbia*

Vasa Radonić – *University of Novi Sad, BioSense Institute, 21000 Novi Sad, Serbia*

Branimir Bajac – *University of Novi Sad, BioSense Institute, 21000 Novi Sad, Serbia*

Complete contact information is available at: https://pubs.acs.org/10.1021/acsomega.4c01599

Author Contributions

B.B., J.S., and V.R. conceived the idea and designed the experiments. S.J. contributed to material preparation (PEI-SWCNT film) and structural and electrical characterization. I.K. and I.M. contributed to immunosensor construction, bacteria cultivation, and electrochemical analysis. I.K., I.M.,

https://doi.org/10.1021/acsomega.4c01599
ACS Omega 2024, 9, 22277–22284

and S.J. processed and analyzed the data. I.K. and S.J. wrote the manuscript.

Funding

This research was funded by the Science Fund of the Republic of Serbia, #Grant No. 7750276, Microfluidic lab-on-a-chip platform for fast detection of pathogenic bacteria using novel electrochemical aptamer-based biosensors—MicroLabAptaSens.

Notes

The authors declare no competing financial interest.

■ ACKNOWLEDGMENTS

This research was supported by the ANTARES project that has received funding from the European Union's Horizon 2020 research and innovation programme under grant agreement SGA-CSA No. 739570 under FPA No. 664387 and the Ministry of Science, Technological Development and Innovation 451-03-47/2023-01/200358.

■ REFERENCES

(1) Zhang, G.; Ma, L.; Beuchat, L. R.; Erickson, M. C.; Phelan, V. H.; Doyle, M. P. Lack of internalization of *Escherichia coli* O157:H7 in lettuce (Lactuca sativa L.) after leaf surface and soil inoculation. *J. Food Prot.* **2009**, *72* (10), 2028−2037.

(2) https://www.ncbi.nlm.nih.gov/books/NBK507845/.

(3) Machado-Moreira, B.; Richards, K.; Abram, F.; Brennan, F.; Gaffney, M.; Burgess, C. M. Survival of *Escherichia coli* and Listeria innocua on Lettuce after Irrigation with Contaminated Water in a Temperate Climate. *Foods* **2021**, *10* (9), No. 2072, DOI: 10.3390/foods10092072.

(4) Zhang, J.; Huang, H.; Song, G.; Huang, K.; Luo, Y.; Liu, Q.; et al. Intelligent biosensing strategies for rapid detection in food safety: A review. *Biosens. Bioelectron.* **2022**, *202*, No. 114003.

(5) Rizzotto, F.; Khalife, M.; Hou, Y.; Chaix, C.; Lagarde, F.; Scaramozzino, N.; Vidic, J. Recent advances in electrochemical biosensors for food control. *Micromachines* **2023**, *14* (7), No. 1412, DOI: 10.3390/mi14071412.

(6) Naresh, V.; Lee, N. A Review on Biosensors and Recent Development of Nanostructured Materials-Enabled Biosensors. *Sensors* **2021**, *21* (4), No. 1109, DOI: 10.3390/s21041109.

(7) Abbas, N.; Song, S.; Chang, M.-S.; Chun, M.-S. Point-of-Care Diagnostic Devices for Detection of *Escherichia coli* O157:H7 Using Microfluidic Systems: A Focused Review. *Biosensors* **2023**, *13* (7), No. 741, DOI: 10.3390/bios13070741.

(8) Pebdeni, A. B.; Roshani, A.; Mirsadoughi, E.; Behzadifar, S.; Hosseini, M. Recent advances in optical biosensors for specific detection of *E. coli* bacteria in food and water. *Food Control* **2022**, *135*, No. 108822.

(9) Liu, B.; Zhuang, J.; Wei, G. Recent advances in the design of colorimetric sensors for environmental monitoring. *Environ. Sci.: Nano.* **2020**, *7* (8), 2195−2213.

(10) Dayal, H.; Ng, W. Y.; Lin, X. H.; Li, S. F. Y. Development of a hydrophilic molecularly imprinted polymer for the detection of hydrophilic targets using quartz crystal microbalance. *Sens. Actuators, B* **2019**, *300*, No. 127044.

(11) Wang, B.; Wang, H.; Lu, X.; Zheng, X.; Yang, Z. Recent advances in electrochemical biosensors for the detection of foodborne pathogens: current perspective and challenges. *Foods* **2023**, *12* (14), No. 2795, DOI: 10.3390/foods12142795.

(12) Curulli, A. Electrochemical biosensors in food safety: challenges and perspectives. *Molecules* **2021**, *26* (10), No. 2940, DOI: 10.3390/molecules26102940.

(13) Podunavac, I.; Kukkar, M.; Léguillier, V.; Rizzotto, F.; Pavlovic, Z.; Janjušević, L.; et al. Low-cost goldleaf electrode as a platform for *Escherichia coli* immunodetection. *Talanta* **2023**, *259*, No. 124557.

(14) Bobrinetskiy, I.; Radovic, M.; Rizzotto, F.; Vizzini, P.; Jaric, S.; Pavlovic, Z.; et al. Advances in Nanomaterials-Based Electrochemical Biosensors for Foodborne Pathogen Detection. *Nanomaterials* **2021**, *11* (10), No. 2700, DOI: 10.3390/nano11102700.

(15) Chen, S.; Yu, Z.; Wang, Y.; Tang, J.; Zeng, Y.; Liu, X.; Tang, D. Block-Polymer-Restricted Sub-nanometer Pt Nanoclusters Nanozyme-Enhanced Immunoassay for Monitoring of Cardiac Troponin I. *Anal. Chem.* **2023**, *95* (38), 14494−14501.

(16) Rathinavel, S.; Priyadharshini, K.; Panda, D. A review on carbon nanotube: An overview of synthesis, properties, functionalization, characterization, and the application. *Mater. Sci. Eng., B* **2021**, *268*, No. 115095.

(17) Balasubramanian, K.; Burghard, M. Biosensors based on carbon nanotubes. *Anal. Bioanal. Chem.* **2006**, *385* (3), 452−468.

(18) Sireesha, M.; Babu, V. J.; Kiran, A. S. K.; Ramakrishna, S. A review on carbon nanotubes in biosensor devices and their applications in medicine. *Nanocomposites* **2018**, *4* (2), 36−57, DOI: 10.1080/20550324.2018.1478765.

(19) Thirumalai, D.; Subramani, D.; Yoon, J.-H.; Lee, J.; Paik, H.; Chang, S.-C. De-bundled single-walled carbon nanotube-modified sensors for simultaneous differential pulse voltammetric determination of ascorbic acid, dopamine, and uric acid. *New J. Chem.* **2018**, *42* (4), 2432−2438.

(20) Ferrier, D. C.; Honeychurch, K. C. Carbon Nanotube (CNT)-Based Biosensors. *Biosensors* **2021**, *11* (12), No. 486, DOI: 10.3390/bios11120486.

(21) Magar, H. S.; Ghica, M. E.; Abbas, M. N.; Brett, C. M. A. A novel sensitive amperometric choline biosensor based on multiwalled carbon nanotubes and gold nanoparticles. *Talanta* **2017**, *167*, 462−469.

(22) Hrapovic, S.; Liu, Y.; Male, K. B.; Luong, J. H. T. Electrochemical biosensing platforms using platinum nanoparticles and carbon nanotubes. *Anal. Chem.* **2004**, *76* (4), 1083−1088.

(23) Chen, C.; Ran, R.; Yang, Z.; Lv, R.; Shen, W.; Kang, F.; Huang, Z. H. An efficient flexible electrochemical glucose sensor based on carbon nanotubes/carbonized silk fabrics decorated with Pt microspheres. *Sens. Actuators, B* **2018**, *256*, 63−70.

(24) Yang, K.; Zhang, C. Simple detection of nucleic acids with a single-walled carbon-nanotube-based electrochemical biosensor. *Biosens. Bioelectron.* **2011**, *28* (1), 257−262.

(25) Chen, M.; Wu, D.; Tu, S.; Yang, C.; Chen, D.; Xu, Y. A novel biosensor for the ultrasensitive detection of the lncRNA biomarker MALAT1 in non-small cell lung cancer. *Sci. Rep.* **2021**, *11* (1), No. 3666.

(26) Sabahi, A.; Salahandish, R.; Ghaffarinejad, A.; Omidinia, E. Electrochemical nano-genosensor for highly sensitive detection of miR-21 biomarker based on SWCNT-grafted dendritic Au nanostructure for early detection of prostate cancer. *Talanta* **2020**, *209*, No. 120595.

(27) Riberi, W. I.; Tarditto, L. V.; Zon, M. A.; Arévalo, F. J.; Fernández, H. Development of an electrochemical immunosensor to determine zearalenone in maize using carbon screen printed electrodes modified with multi-walled carbon nanotubes/polyethyleneimine dispersions. *Sens. Actuators, B* **2018**, *254*, 1271−1277.

(28) Malhotra, R.; Patel, V.; Vaqué, J. P.; Gutkind, J. S.; Rusling, J. F. Ultrasensitive electrochemical immunosensor for oral cancer biomarker IL-6 using carbon nanotube forest electrodes and multilabel amplification. *Anal. Chem.* **2010**, *82* (8), 3118−3123.

(29) Thapa, A.; Soares, A. C.; Soares, J. C.; Awan, I. T.; Volpati, D.; Melendez, M. E.; et al. Carbon Nanotube Matrix for Highly Sensitive Biosensors To Detect Pancreatic Cancer Biomarker CA19−9. *ACS Appl. Mater. Interfaces* **2017**, *9* (31), 25878−25886.

(30) Wan, Y.; Deng, W.; Su, Y.; Zhu, X.; Peng, C.; Hu, H.; et al. Carbon nanotube-based ultrasensitive multiplexing electrochemical immunosensor for cancer biomarkers. *Biosens. Bioelectron.* **2011**, *30* (1), 93−99.

(31) Stanojev, J.; Bajac, B.; Cvejic, Z.; Matovic, J.; Srdic, V. V. Development of MWCNT thin film electrode transparent in the mid-IR range. *Ceram. Int.* **2020**, *46* (8), 11340−11345.

(32) Stanojev, J.; Armaković, S.; Joksović, S.; Bajac, B.; Matović, J.; Srdić, V. V. Comprehensive Study of the Chemistry behind the Stability of Carboxylic SWCNT Dispersions in the Development of a Transparent Electrode. *Nanomaterials* **2022**, *12* (11), No. 1901, DOI: 10.3390/nano12111901.
(33) Lazanas, A. C.; Prodromidis, M. I. Electrochemical impedance spectroscopy—a tutorial. *ACS Meas. Au* **2023**, *3*, 162−193, DOI: 10.1021/acsmeasuresciau.2c00070.
(34) Yan, X.; Suzuki, T.; Kitahama, Y.; Sato, H.; Itoh, T.; Ozaki, Y. A study on the interaction of single-walled carbon nanotubes (SWCNTs) and polystyrene (PS) at the interface in SWCNT-PS nanocomposites using tip-enhanced Raman spectroscopy. *Phys. Chem. Chem. Phys.* **2013**, *15* (47), 20618−20624.
(35) Müller, C.; Al-Hamry, A.; Kanoun, O.; Rahaman, M.; Zahn, D. R. T.; Matsubara, E. Y.; Rosolen, J. M. Humidity Sensing Behavior of Endohedral Li-Doped and Undoped SWCNT/SDBS Composite Films. *Sensors* **2019**, *19* (1), No. 171, DOI: 10.3390/s19010171.
(36) Long, G. L.; Winefordner, J. D. Limit of detection. A closer look at the IUPAC definition. *Anal. Chem.* **1983**, *55* (7), 712A−724A, DOI: 10.1021/ac00258a001.
(37) Doyle, M. P. Food safety: bacterial contamination. In *Encyclopedia of Human Nutrition*; Elsevier, 2013; pp 322−330.
(38) Sidhu, R. K.; Cavallaro, N. D.; Pola, C. C.; Danyluk, M. D.; McLamore, E. S.; Gomes, C. L. Planar Interdigitated Aptasensor for Flow-Through Detection of Listeria spp. in Hydroponic Lettuce Growth Media. *Sensors* **2020**, *20* (20), No. 5773, DOI: 10.3390/s20205773.
(39) Zhang, M.; Chen, Y.; Liu, S. G.; Shi, X. Highly sensitive detection of *L.monocytogenes* using an electrochemical biosensor based on Si@MB/AuNPs modified glassy carbon electrode. *Microchem. J.* **2023**, *194*, No. 109357.
(40) El-Moghazy, A. Y.; Wisuthiphaet, N.; Yang, X.; Sun, G.; Nitin, N. Electrochemical biosensor based on genetically engineered bacteriophage T7 for rapid detection of *Escherichia coli* on fresh produce. *Food Control* **2022**, *135*, No. 108811.
(41) https://www.dropsens.com/en/screen_printed_electrodes_pag.html.
(42) https://www.palmsens.com/products/sensors/?utm_source=google_ads&utm_medium=cpc&utm_campaign=sensors&gad_source=1&gclid=CjwKCAiAg9urBhB_EiwAgw88mQyQ90XNbz2M-q c Z u Y t V O L y 6 4 x X u C S P 7 c 7 M 8 K W b n h Z 9 g - yY8PEkS7BoC7QMQAvD_BwE.

https://doi.org/10.1021/acsomega.4c01599
ACS Omega 2024, 9, 22277−22284